JOURNAL OF COMPUTATIONAL PHYSICS 73, 380–394 (1987)

Computation of Free-Surface Flows

N. S. ASAITHAMBI

Department of Mathematics and Statistics, Mississippi State University, Mississippi State, Mississippi 39762

Received April 25, 1986; revised February 13, 1987

Free-surface flows define an area of a great deal of engineering interest. In this paper, we present a finite-difference method for an accurate and efficient solution of potential flows with a free surface. Boundary-fitted coordinates are used to eliminate the difficulty introduced by the free surface. The method is illustrated with applications to problems involving unsteady two-dimensional flows. © 1987 Academic Press, Inc.

1. INTRODUCTION

A free-surface flow problem is a problem of fluid flow involving differential equations on fluid domains, parts of whose boundaries, identified as the free surface of the fluid, are unknown and must be determined as part of the solution. In this paper, a class of free-surface flows, for which the unsteady two-dimensional surface waves serve as a model, are considered. The numerical method of this paper eliminates the difficulty involving the unknown free surface by imposing boundary conditions on a known boundary in a mapped domain.

Several numerical methods are now available for the computation of potential flows with a free surface. A survey of these methods can be found in Yeung [7]. The numerical method of this paper is one of the first attempts to use implicit finite-difference schemes for nonlinear free-surface computations. The primary features of the method include the use of boundary-fitted coordinates and imposing the boundary conditions on the free surface in their full nonlinear form. The method can be used for a class of free-surface problems characterized by the following property:

> The fluid domain has an unknown boundary on which a nonlinear double condition has to be imposed. There is a "time-like" variable which is used as the marching variable of the finite-difference procedure, and it appears only in the double-condition. An elliptic equation independent of the marching variable holds in the fluid domain.

Numerical results are presented for problems with this property.

Applications

Certain three-dimensional steady free-surface flows can be described by a system of equations similar to the system governing unsteady two-dimensional surface

0021-9991/87 $3.00

waves. Examples are flows involving "slender" geometries such as slender jets, channels of slowly varying width, slender ships. The slenderness will permit us to consider one coordinate direction as the "time-like" variable and march along this direction.

The numerical method described in this paper has also been applied to three-dimensional steady flows with a free surface. In particular, computations are carried out for two problems. The first problem attempted is the computation of flows in channels of varying width. The second problem is the computation of flows past slender ships. The problems considered are simplified versions of real-life situations. However, the numerical results obtained are encouraging. The success of the method of these problems indicates the possibility of employing the method to attack a wide variety of water wave problems.

2. Governing Equations

We consider the full, time-dependent, nonlinear equations for water waves in two dimensions. The fluid motion is assumed to be irrotational, and the fluid to be inviscid and incompressible. Surface tension effects are neglected. Let Oxy be a fixed coordinate system in which the Ox axis coincides with the bottom surface $\mathscr{B}$ of the fluid which is assumed to be horizontal. The y axis points vertically upwards. The free-surface $\mathscr{F}$ of the fluid is denoted by its elevation which is described as $y = \Gamma(x, t)$. Figure 1 shows the physical situation. The fluid disturbance at time t is described by a velocity potential $\phi(x, y, t)$ with the fluid velocity u given by $\nabla\phi$. The potential ϕ satisfies the Laplace equation in the fluid domain Ω, and the momentum equations yield Bernoulli's integral. Hence,

$$\nabla^2\phi(x, t) = 0 \qquad \text{for} \quad x = (x, y) \text{ in } \Omega \tag{2.1}$$

$$\frac{p(x, t)}{\rho} + \phi_t + \frac{1}{2}|\nabla\phi|^2 + gy = gh_0, \tag{2.2}$$

where,

p is the fluid pressure

ρ is the density

g is the acceleration due to gravity

h_0 is the height of the undisturbed surface.

For the surface-wave problem in two dimensions, the system of equations to be solved is expressed as

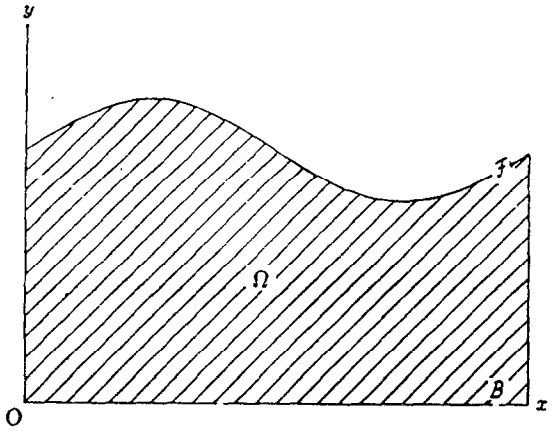

FIG. 1. Surface waves.

$$\nabla^2\phi = 0 \qquad \text{in } \Omega \tag{2.3}$$

$$\Gamma_t + \Gamma_x\phi_x - \phi_y = 0 \qquad \text{on } y = \Gamma$$
$$\phi_t + \tfrac{1}{2}(\phi_x^2 + \phi_y^2) + g\Gamma = gh_0 \qquad \text{on } y = \Gamma \tag{2.4}$$

$$\phi_y = 0 \qquad \text{on } y = 0. \tag{2.5}$$

Once ϕ is determined, Eq. (2.2) can be used to evaluate $p(x, t)$.

3. Boundary-Fitted Coordinates

The accuracy of boundary conditions in fluid flow problems is very important for the accuracy of the entire flow computation. However, for free-surface flows, since the boundary is determined as part of the solution, numerical methods encounter difficulties in imposing the boundary conditions accurately. The use of boundary-fitted coordinates will help overcome these difficulties.

The basic idea of boundary-fitted coordinates is to transform any given arbitrary domain into regions composed of rectangles so that the physical boundaries of the problem are mapped to coordinate lines in the mapped space. This feature in the numerical methods makes it easy to implement finite-difference schemes.

For the surface-wave problem in two dimensions the transformation

$$\begin{aligned} \xi &= x \\ \eta &= y/\Gamma(x, t) \\ \tau &= t \end{aligned} \tag{3.1}$$

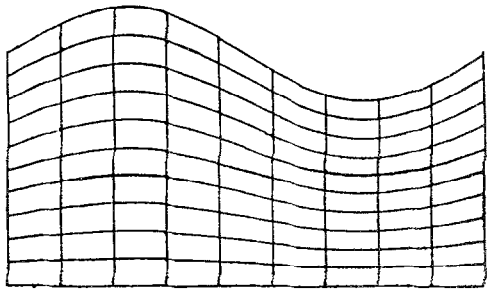

FIG. 2. Boundary-fitted grid.

yields a system of boundary-fitted coordinates. Figure 2 shows a grid system in the physical domain that was obtained using a rectangular grid in the mapped domain. Now the system of Eqs. (2.3)–(2.5) gets transformed to

$$A\phi_{\xi\xi} - 2\eta B\phi_{\xi\eta} + \frac{C}{H}\phi_{\eta\eta} - \eta D\phi_{\eta} = 0 \tag{3.2}$$

$$\begin{aligned} H_\tau + H_\xi\phi_\xi - C\phi_\eta &= 0 \qquad \text{on } \eta = 1 \\ \phi_\tau + \frac{1}{2}\phi_\xi^2 - \frac{1}{2}\frac{C}{H}\phi_\eta^2 + gH &= gh_0 \qquad \text{on } \eta = 1 \end{aligned} \tag{3.3}$$

$$\phi_\eta = 0 \qquad \text{on } \eta = 0 \tag{3.4}$$

in the mapped domain. In (3.2)–(3.4), $A = 1$, $B = H_\xi/H$, $C = (1 + \eta^2 H_\xi^2)/H$, and $D = B_\xi - B^2$.

4. Numerical Method

The governing equations for the free-surface flows of interest to us possess the following form in the computational domain (ξ, η, τ):

$$\mathbb{P}\phi(\xi, \eta) = f \tag{4.1}$$

$$\begin{aligned} H_\tau &= f_1(H, H_\xi, \phi_\xi, \phi_\eta) \qquad \text{on } \eta = 1 \\ \phi_\tau &= f_2(H, H_\xi, \phi_\xi, \phi_\eta) \qquad \text{on } \eta = 1 \end{aligned} \tag{4.2}$$

$$\phi_\eta = 0 \qquad \text{on } \eta = 0, \tag{4.3}$$

where $\mathbb{P}$ is an elliptic operator and (4.2) is a system of nonlinear differential equations for H and ϕ on the boundary $\eta = 1$. Equation (4.3) holds on $\eta = 0$. Here, the boundaries $\eta = 1$ and $\eta = 0$ correspond to the free surface and the bottom surface of the fluid, respectively.

The basic approach of the numerical method is to first consider H and ϕ as functions of ξ and τ alone defined on the line $\eta = 1$ and solve the system of Eq. (4.2) subject to the auxiliary condition (4.1) in the interior. The condition (4.1) is used to determine ϕ_η on $\eta = 1$ which is required in the system (4.2). The problem now is to determine H and ϕ for all τ starting with appropriate initial values for H and ϕ at an initial $\tau = \tau_0$.

Solving for ϕ in the interior, i.e., solving Eq. (4.1) will essentially involve an iterative scheme. Since the boundary conditions are nonlinear, their discretization will also require an iterative scheme for their solution. In the present numerical method, the boundary and the interior computations are performed alternatively during each iteration. In other words, the boundary and interior iterative procedures are coupled so that both the boundary and the interior values obtained for ϕ are improved simultaneously.

Finite Difference Scheme

The computational domain is represented by a grid system (ξ_i, η_j, τ_n), where

$$\begin{aligned} \xi_i &= (i-1)\,\Delta\xi & i &= 1, 2, \ldots, N \\ \eta_j &= 1-(j-1)\,\Delta\eta & j &= 1, 2, \ldots, M \\ \tau_n &= n\,\Delta\tau & n &= 0, 1, 2, \ldots, \end{aligned}$$

with $\Delta\xi = 1/(N-1)$, $\Delta\eta = 1/(M-1)$, and $\Delta\tau$ chosen to satisfy appropriate accuracy criteria.

With $w := (H, \phi_s)^{\mathrm{T}}$, where ϕ_s denotes the potential ϕ on the boundary $\eta = 1$ one can write the system (4.2) in the form

$$w_\tau = F(w, w_\xi, \phi_\eta). \tag{4.4}$$

A second-order accurate Crank–Nicolson discretization of (4.4) is written as

$$w^{n+1} = w^n + \frac{1}{2}\Delta\tau(F^{n+1} + F^n), \tag{4.5}$$

where the superscripts n and $n+1$ denote evaluation at τ_n and τ_{n+1}, respectively. However, Eq. (4.5) involves nonlinear terms which will complicate the numerical procedure if used directly. Therefore, a form which is somewhat easier to deal with numerically and yet maintains the second-order accuracy is obtained in the following manner. Define

$$\begin{gathered} p := w_\xi, \qquad q := \phi_\eta \\ D_n F^m(w, p, q) := F_w(\tau_n)\, w^m + F_p(\tau_n)\, p^m + F_q(\tau_n)\, q^m \\ \Delta F^n := D_n F^{n+1} - D_n F^n \end{gathered} \tag{4.6}$$

Then $F^{n+1} := F(w^{n+1}, p^{n+1}, q^{n+1})$ is obtained by a Taylor's series expansion as

$$F^{n+1} = F^n + \Delta F^n. \tag{4.7}$$

Now (4.5) takes the form

$$w^{n+1} = w^n + \Delta\tau\, F^n + \tfrac{1}{2}\Delta\tau\, \Delta F^n, \tag{4.8}$$

which can be rewritten in the form

$$(I - \tfrac{1}{2}\Delta\tau\, F_w(\tau_n))\, w^{n+1} - \tfrac{1}{2}\Delta\tau\, F_p(\tau_n)\, p^{n+1} = \delta^{n+1}, \tag{4.9}$$

where

$$\delta^{n+1} = w^n + F^n\, \Delta\tau - \tfrac{1}{2}\Delta\tau\, D_n F^n + \tfrac{1}{2}\Delta\tau\, F_q(\tau_n)\, q^{n+1} \tag{4.10}$$

and (4.9) is obtained on substituting for ΔF^n in (4.8) from (4.6).

Now $p := w_\xi$ has to be discretized and we use the central-difference formula

$$p_1^n = (w_{i+1}^n - w_{i-1}^n)/2\Delta\xi, \qquad i = 2, 3, \ldots, N-1, \tag{4.11}$$

to obtain

$$X_i w_{i-1}^{n+1} + Y_i w_i^{n+1} + Z_i w_{i+1}^{n+1} = \delta_i^{n+1} \tag{4.12}$$

with

$$X_i = \tfrac{1}{4}\lambda F_p(\tau_n), \qquad Y_i = I - \tfrac{1}{2}\Delta\tau\, F_w(\tau_n), \qquad Z_i = -X_i \tag{4.13}$$

and

$$\lambda = \Delta\tau/\Delta\xi.$$

The linear system of Eqs. (4.12) will be closed by using appropriate boundary conditions corresponding to $i = 1$ and $i = N$.

The linear system of Eqs. (4.12) describes the kinematic and dynamic conditions on the unknown boundary in the physical domain. However, the right-hand side of (4.12) contains the terms q_i^{n+1} and q_i^n which can be computed only after the potential ϕ has been determined in the interior. Here, q_i^n is an approximation to ϕ_η on $y = 1$, $\xi = \xi_i$, and $\tau = \tau_n$. It is computed using the formula

$$(\phi_\eta)_i^n = (3\phi_{i1}^n - 4\phi_{i2}^n + \phi_{i3}^n)/2\Delta\eta \tag{4.14}$$

which is second-order accurate. The term q_i^{n+1} is unknown when the boundary values are solved for, since it will involve ϕ_{i1}^{n+1}, ϕ_{i2}^{n+1}, and ϕ_{i3}^{n+1} in its computation. At any iteration in solving for ϕ in the interior, approximate values of ϕ_{i1}^{n+1}, ϕ_{i2}^{n+1},

and ϕ_{i3}^{n+1} will be available. Therefore, the boundary system of Eqs. (4.12) can be solved after every iteration for the solution of ϕ in the interior and successive improvements for the boundary and the interior can be obtained simultaneously.

Solution of ϕ in the Interior

The most general form of the elliptic equation (4.1) for problems of interest to us is

$$A\phi_{\xi\xi} - 2B\phi_{\xi\eta} + C\phi_{\eta\eta} = D\phi_{\xi} + E\phi_{\eta}, \tag{4.15}$$

where the coefficients A, B, C, D, and E are functions of ξ, η, and the free-surface elevation. Equation (4.15) can be discretized in the form

$$P_h\phi_{i,j} = 0, \tag{4.16}$$

where P_h is the discrete equivalent of the elliptic operator $\mathbb{P}$ of (4.1), obtained by using second-order accurate difference formulas for the partial derivatives

$$\begin{aligned}
\phi_{\xi\xi} &= (\phi_{i-1,j} - 2\phi_{i,j} + \phi_{i+1,j})/(\Delta\xi)^2 \\
\phi_{\xi\eta} &= (\phi_{i+1,j-1} - \phi_{i-1,j-1} - \phi_{i+1,j+1} + \phi_{i-1,j+1})/2\Delta\xi\,\Delta\eta \\
\phi_{\eta\eta} &= (\phi_{i,j-1} - 2\phi_{i,j} + \phi_{i,j+1})/(\Delta\eta)^2 \\
\phi_{\xi} &= (\phi_{i+1,j} - \phi_{i-1,j})/2\Delta\xi \\
\phi_{\eta} &= (\phi_{i,j-1} - \phi_{i,j+1})/2\Delta\eta.
\end{aligned} \tag{4.17}$$

The subscripts i and j denote evaluation at the point (ξ_i, η_j). The resulting linear system of equations is then solved by an iterative scheme such as the line-successive over relaxation (line SOR).

The computational algorithm based on the finite-difference scheme of this section is given below.

ALGORITHM [to compute the free-surface height and the potential for a free-surface flow problem by a marching procedure].

1. [Initialize] $n := 0$; $\tau := \tau_0$; initialize Γ, ϕ on $\eta = 1$.
2. [ϕ inside] Solve (4.16) to initialize ϕ in the interior.
3. [Start loop] $k := 0$; initialize ϕ^{n+1}.
4. [Boundary] Solve (4.12) to obtain Γ and ϕ_s.
5. [Interior] Perform one sweep of line-SOR on (4.16).
6. [Exit?] Exit if tolerance is met; else $k := k + 1$; go to 4
7. [Advance] $n := n + 1$; $\tau := \tau_n$
8. [Stop?] Stop if $\tau_n > \tau_{\max}$; else go to 3.

5. Programming Considerations

A. *Boundary Conditions*

In solving free-surface problems on domains of infinite extent, one needs to keep the computational region finite. This makes it necessary to work with a fixed boundary and prescribe appropriate boundary conditions at the computational boundary.

For periodic free-surface waves, one can study the waves through a window of length equal to one wavelength by imposing the periodicity conditions at the ends. Periodic boundary conditions give rise to systems of linear equations whose coefficient matrices are almost tridiagonal; i.e., the first and the last rows have an additional entry in their last and first columns, respectively. In order to preserve and take advantage of the tridiagonal structure of the coefficient matrices, a modified version of a tridiagonal system solver is used. A discussion of the modification is given in Asaithambi [1].

Radiation-type boundary conditions can be used for unsteady flows when there is an open boundary. For steady flows, however, radiation-type conditions are not widely known.

B. *Initial Iterate for Laplacian Solver*

Sometimes the iterative procedure for the Laplacian may take a long time to converge if the initial iterate is too far from the solution. To make sure that the initial iterate is reasonably close to the solution, a linear extrapolation in τ is used to obtain the first iterate. In particular, the values $\phi_{i,j}^{n+1,0}$ are obtained as

$$\phi_{i,j}^{n+1,0} = 2\phi_{i,j}^{n} - \phi_{i,j}^{n-1} \tag{5.1}$$

for the interior values. The boundary values are obtained from the Crank–Nicolson marching step. It has been observed that the number of iterations was reduced considerably when (5.1) was used instead of merely setting

$$\phi_{i,j}^{n+1,0} = \phi_{i,j}^{n}. \tag{5.2}$$

The additional storage required to hold $\phi_{i,j}^{n-1}$ is thus justified. This technique was used in [4] and found to work satisfactorily.

C. *Treatment of Nonlinear Terms*

Earlier, it was mentioned that the scheme (4.5) involves nonlinear terms and will complicate the numerical method if used directly. It turns out that it does not actually complicate the method, but only makes it slow. However, a close look at the scheme with the nonlinear terms taken into account as they appear, indicates that the present approach has led to a more efficient way of dealing with the computations. For instance, if one uses a method like Newton's method to solve the nonlinear equations (4.5), the resulting linear system of equations will still be

tridiagonal, but the coefficient matrices X_i, Y_i, and Z_i will have to be evaluated at τ_{n+1} instead of τ_n as in (4.13), and this would mean that they have to be computed at each iteration. For a large number of grid points on the free surface, one would then spend a lot of time computing the coefficient matrices.

6. Numerical Results

The numerical method of Section 4 was obtained as an improvement over a similar method developed by Strikwerda and Geer [4] for computing the shape of freely falling jets. The desired improvement in terms of computational effort has been achieved and the present numerical method can be shown to be formally second-order accurate. Since the finite-difference form used is implicit, it is unconditionally stable for linear problems. In this section we present the numerical results obtained by using the method of Section 4 for computing free-surface flows in two dimensions.

Order of Accuracy

In order to illustrate the second-order accuracy of the method by a numerical example, the following problem has been solved. Two functions $h(x, t)$ and $\phi(x, y, t)$ are sought which satisfy

$$\nabla^2\phi = 0 \qquad \text{in} \quad \{0 \leqq x \leqq 1,\ 0 \leqq y \leqq h(x, t)\} \tag{6.1}$$

$$\begin{aligned} h_t + h_x\phi_x - \phi_y &= f_1(x, h, t) \\ \phi_t + \tfrac{1}{2}(\phi_x^2 + \phi_y^2) + gh &= f_2(x, h, t) \end{aligned} \tag{6.2}$$

$$h, \phi \qquad \text{periodic in } x \text{ with period unity.} \tag{6.3}$$

The functions f_1 and f_2 in (6.2) are chosen so that the solutions h and ϕ are simple smooth functions. Then the numerical computation consists in recovering h and ϕ as solutions of (6.1)–(6.3). The errors in h and ϕ can then be computed and the order of the numerical method determined by computing with various mesh sizes.

The numerical results are obtained for the choices

$$h(x, t) = 1 + A \sin \omega(x - ct),$$

$$\phi(x, y, t) = B \cos \omega(x - ct) \cosh \omega y.$$

The corresponding f_1 and f_2 can be obtained by simply substituting for h and ϕ on the left-hand sides of (6.2). In the above choices for h and ϕ, A, B, and c are arbitrary constants. The algorithm was tested with the above choices for h and ϕ for various choices of the grid-parameters N, M, and $\Delta\tau$. The choices for A, B, c, and ω were: $A = 0.001$, $B = 0.001$, $c = 1.0$, $\omega = 2\pi$. For all computations for which results

appear below, $N = M$, $\Delta\tau = 1/(N-1)$, and marching is carried through $\tau = 0.5$. The number of grid points in the ξ direction was varied as 21, 41, 51, and 61 and the tolerance ε for the SOR procedure was chosen as 10^{-5}. Table I shows the errors in h and ϕ measured in the l^2 norm. The columns entitled "order" indicate the order of accuracy of the method. The entries in these columns are obtained using the formula

$$\text{order} = (\log(e_{N_1}) - \log(e_{N_2}))/(\log(N_1) - \log(N_2)), \tag{6.4}$$

where e_N denotes the error in h or ϕ with computations performed on a $N \times N$ grid. The closeness of the entries in the third and fifth columns to -2 indicates that the overall accuracy of the method is second order.

Transient Surface-Wave Problems

Numerical results are presented for two specific instances of two-dimensional transient surface waves and the computational results are compared with previously obtained analytical results.

A. *Standing Waves*

In this subsection, numerical results for the computation of standing waves of finite amplitude in water of uniform depth are presented. The initial conditions for this problem are obtained from the approximate analytical solution of Tadjbakhsh and Keller [5], and the computed solution is compared with the approximate analytical one. Tadjbakhsh and Keller sought a solution to this problem in the form of an expansion in powers of the amplitude of the linearized surface wave. They solved the problem based on the following formulation:

$$\nabla^2\phi = 0 \qquad \text{in} \quad \{0 \leqq x \leqq \pi,\ -d \leqq y \leqq s\eta\} \tag{6.5}$$

$$\begin{aligned} \omega\eta_t + s\eta_x\psi_x - \psi_y &= 0 \qquad \text{on} \quad y = s\eta \\ \omega\psi_t + \tfrac{1}{2}s(\psi_x^2 + \psi_y^2) + \eta &= 0 \qquad \text{on} \quad y = s\eta \end{aligned} \tag{6.6}$$

$$\psi_n = 0 \qquad \text{on} \quad y = -d,\ x = 0,\ \pi \tag{6.7}$$

$$2s = \eta(0, 0) - \eta(\pi, 0). \tag{6.8}$$

TABLE I

$N-1$	$h_{\text{err}}(\times 10^{-4})$	Order	$\phi_{\text{err}}(\times 10^{-7})$	Order
20	6.21	—	38.5	—
40	1.56	−2.06	9.57	−2.06
50	1.00	−2.03	6.12	−2.05
60	0.70	−2.03	4.25	−2.04

Their solution is described by

$$\begin{aligned} s\eta &= s\eta^{(0)} + s^2\eta^{(1)} + \tfrac{1}{2}s^3\eta^{(2)} + O(s^4) \\ s\psi &= s\psi^{(0)} + s^2\psi^{(1)} + \tfrac{1}{2}s^3\psi^{(2)} + O(s^4) \\ \omega &= \omega_0 + \tfrac{1}{2}s^2\omega_2 + O(s^3) \end{aligned} \tag{6.9}$$

In (6.5)–(6.9), $y = -d$ denotes the bottom of the fluid, $y = 0$ denotes the undisturbed surface of the fluid, and $s\eta$ denotes a small disturbance about the undisturbed fluid-surface, where s is the steepness of the waves multiplied by π. The waves are assumed periodic both in space and time. The period in space is 2π, and ω, the temporal frequency, is sought as part of the solution. In particular, Tadjbakhsh and Keller found that

$$\begin{aligned} \omega_0^2 &= \tanh d \\ \omega_2 &= (9\omega_0^{-7} - 12\omega_0^{-3} - 3\omega_0 - 2\omega_0^5)/32. \end{aligned} \tag{6.10}$$

By examining (6.10) they found that ω increases with s for $d < d^*$, where $d^* \approx 1.07$ and decreases with increasing s for $d > d^*$. Vanden-Broeck and Schwartz [6] have computed these waves by a truncated-Fourier series approximation and concluded that the second-order approximation due to Tadibakhsh and Keller is an excellent approximation for large values of d.

The computed solutions indicate that, for $d = 3$, the surface profile is not much different from the sine wave of linear theory. The nonlinear effects are predominant as d decreases, and the wave develops a narrow crest and a broad trough. Figure 3 shows two different computed profiles for $s = 0.07$ at $t = \pi/2$.

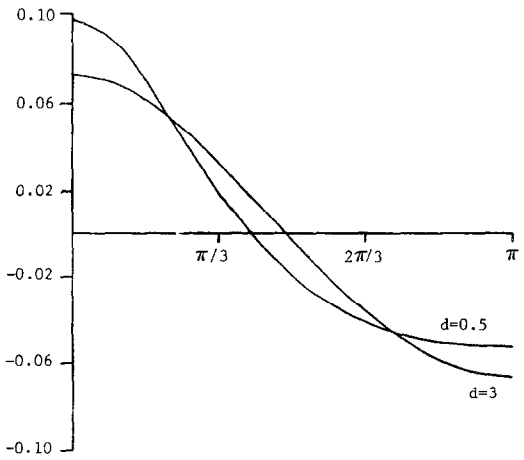

FIG. 3. Free-surface profiles.

The present numerical method is not designed specifically for time-periodic problems. However, since the initial solution could be advanced in time without any difficulty whatsoever, ω, the temporal frequency, could be estimated. For this purpose, the free-surface elevation at $x=0$ is recorded at each time step while marching several periods in time. Figure 4 shows a typical time evolution, and, for comparison purposes, the analytical solution of Tadjbakhsh and Keller is also shown in dotted lines. The nonlinear least-squares program NL2SOL was used to compute an approximation or the form

$$\eta(0, t) = A_0 + \sum_{k=1}^{N} A_k \cos k\omega t + B_k \sin k\omega t. \tag{6.11}$$

The frequency was estimated as 0.866 for $d=1$ and 0.980 for $d=3$, with $s=0.02$, while the corresponding results due to Tadjbakhsh and Keller were 0.873 and 0.999, respectively.

Finally, in Fig. 5, the computed profiles of the standing wave for $s=0.05$ and $d=0.5$ at different times from $t=0$ to $\pi/2$ are presented.

B. *Progressing Waves*

Numerical results for the computation of surface waves progressing at a uniform velocity c are presented in this subsection. The initial conditions for this problem have been obtained from a very accurate solution by Schwartz [3], which is based on Stokes' expansion. The governing equations in the frame of reference moving with the wave are described by

$$\begin{aligned} \Gamma_X \Phi_X - \Phi_Y &= 0 \\ \tfrac{1}{2}(\Phi_X^2 + \Phi_Y^2) + g(\Gamma - h_0) &= \tfrac{1}{2}K, \end{aligned} \tag{6.12}$$

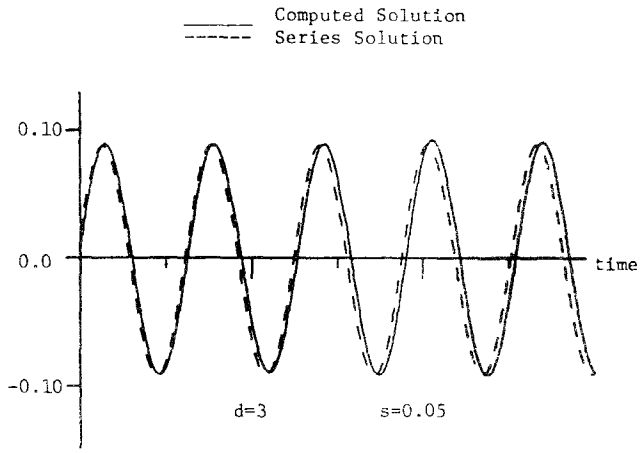

FIG. 4. Surface height as a function of time.

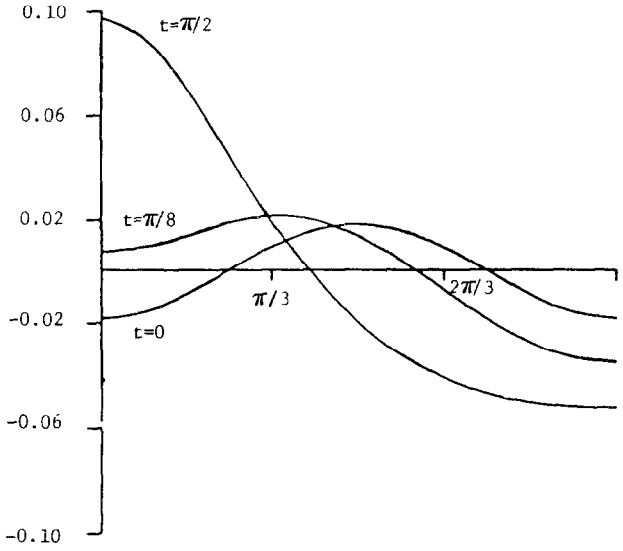

FIG. 5. Free-surface profiles.

where the change of variables,

$$X = x + ct \qquad \text{and} \qquad \Phi = \phi + cX, \tag{6.13}$$

has been used to obtain the steady-state equations. In (6.13), c is called the phase velocity of the progressing waves and K is called the Bernoulli's constant. Schwartz [3] uses two parameters D, the depth of the fluid, and s, the steepness of the waves, to describe the surface profile and the potential. With

$$\sigma_n = 1 + e^{-2nD} \qquad \text{and} \qquad \delta_n = 1 - e^{-2nD}, \tag{6.14}$$

the free-surface profile and the potential are parametrically described by

$$\begin{aligned} X &= -\sum_{n=1}^{\infty} (a_n \sigma_n / n) \sin n\chi - \chi \\ Y &= \sum_{n=1}^{\infty} (a_n \delta_n / n) \cos n\chi \\ \Phi &= -c\chi, \end{aligned} \tag{6.15}$$

where $-\pi \leqq X \leqq \pi$. In (6.15), the coefficients a_n are expressible as series expansions in s, the steepness of the waves, defined as

$$2s := (Y(\chi = \pi) - Y(\chi = 0)). \tag{6.16}$$

The expansions of Schwartz [3] have been used in obtaining an initial profile for the present computations.

The present numerical method was tested on these waves and the numerical results obtained were compared with the accurate solution of Schwartz. For initial conditions, the wave profile and the potential were computed from Schwartz and the solution advanced in time. The time-stepping must translate the waves at an appropriate speed in the proper direction based on the initial conditions. Preliminary computations indicated that the present method does not perform all that well for small values of the depth D of the fluid. But, this is due to the lack of accuracy in the initial conditions, since we have only taken a total of nine expansion coefficients for computing the same. However, for larger values of D, the method gives excellent results. Figure 6 shows both the accurate and the time-stepped profiles at various instants of time, for $s = 0.2$ and $D = 3$. The two profiles are almost indistinguishable, and it is seen that there are no unwarrented oscillations that grow in time, in contrast to the solution obtained by Longuet-Higgins and Cokelet [2]. The velocity of the progressing wave was also computed using NL2SOL, and it was found to be 0.9976 while Schwartz expansions yield a value of 0.9978.

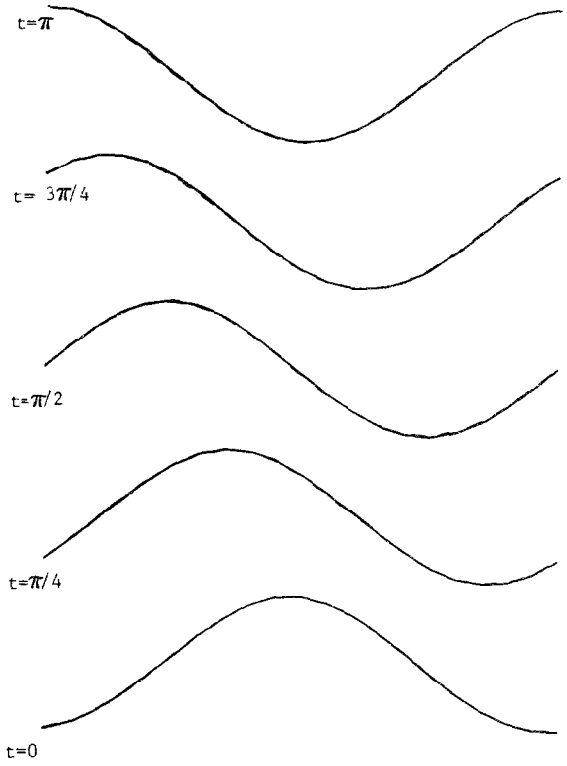

FIG. 6. Stokes' wave profiles.

Accuracy Checks

The computations for the two-dimensional surface wave problems were monitored all the way by incorporating the following accuracy checks:

(i) The average height of the free surface profile must be h_0.

(ii) The sum of the potential and kinetic energies must remain constant at all times.

As an additional check, the reversibility of the system of equations was verified. That is, the system of equations could be solved either in the forward direction or the backward direction. By marching up to a certain time and then marching back to the starting point, the initial conditions could be recovered within the accuracy limits of the method.

7. Conclusions

The numerical method presented here has been shown to be an accurate and efficient method for computing free-surface waves. The method has been shown to be second-order accurate (Table I) and in agreement with analytical methods. The method uses the full nonlinear equations for water waves and hence can be used to study many of the nonlinear phenomena of water waves.

Acknowledgments

The author acknowledges Professor Strikwerda of the Computer Sciences Department at the University of Wisconsin for his guidance and help during this research. The Mathematics Research Center at Wisconsin is acknowledged for providing the computing facilities and the Office of Naval Research for funding this research under Contract N00014-84-K0454. The author appreciates the comments of the reviewers.

References

1. N. S. Asaithambi, Ph. D. dissertation, Computer Sciences Department, University of Wisconsin-Madison, 1985 (unpublished).
2. M. S. Longuet-Higgins and E. D. Cokelet, *Proc. R. Soc. London, Ser. A* **350**, 1 (1976).
3. L. W. Schwartz, *J. Fluid Mech.* **62**, 553 (1974).
4. J. C. Strikwerda and J. F. Geer, *SIAM Sci. Stat. Comput.* **1**, 449 (1980).
5. I. Tadjbakhsh and J. B. Keller, *J. Fluid Mech.* **8**, 442 (1960).
6. J. M. Vanden-Broeck and L. W. Schwartz, *Phys. Fluids* **22**, 1868 (1978).
7. R. W. Yeung, *Annu. Rev. Fluid Mech.* **14**, 395 (1982).